Kinetics of reconstructive austenite to ferrite transformation in low alloy steels

R. C. Reed and H. K. D. H. Bhadeshia

A thermodynamic model has been coupled with simplified kinetic theory, so that, subject to a number of assumptions, the one-dimensional parabolic thickening constant α_1 for allotriomorphic ferrite growing from austenite can be estimated as a function of temperature and composition. To do this, kinetic theory for ternary Fe–C–X systems (where X represents a substantial alloying element) is extended to multicomponent alloys. Values of α_1 calculated assuming local equilibrium and paraequilibrium are compared. Consistent with recent calculations, the slope of the α_1 versus temperature plot is found to change abruptly on entry into the negligible partitioning local equilibrium regime, consistent with an increase in interfacial velocity. At very high supersaturations, the effect of the cross-terms in the diffusivity matrix appears to be small and only then can their effect be ignored. At temperatures below the Ae_3', the value of α_1, calculated assuming local equilibrium, is less than that calculated assuming paraequilibrium. Classical nucleation theory is used to model the ferrite allotriomorphs as discs growing from prior austenite grain boundaries. It has been demonstrated that the model developed here can reproduce the C-curve behaviour typical of those parts of the time–temperature–transformation diagrams that are due to allotriomorphic ferrite, provided the paraequilibrium mode of transformation is assumed to be operative. This work therefore suggests that in multicomponent alloys, the state of true local equilibrium does not exist at the advancing interface. Some problems associated with the paraequilibrium mode of transformation during reconstructive growth are discussed.

MST/1452

 Manuscript received 8 April 1991; in final form 10 February 1992. *At the time the work was carried out the authors were in the Department of Materials Science and Metallurgy, University of Cambridge/JRDC. Dr Reed is now in the Department of Materials, Imperial College of Science, Technology and Medicine, London.*

Introduction

In the past 30 years or so, there has been remarkable progress in the collection and assessment of thermodynamic data for metals and alloys. Such work is near fruition, since there is now available a number of software systems (e.g. Refs. 1, 2) capable of estimating the phase diagram as a function of pressure, temperature, and the combined effect of numerous alloying elements, given a starting set of possible phases.

The ability to predict diagrams in this way is of obvious necessity in the design of new alloys. However, in many applications, metastable phases are present, often because they offer advantageous properties. Indeed, many large scale processes are now tending towards conditions of high supercooling, since it is in those circumstances that ultrafine grained microstructures, phases having non-equilibrium solute concentrations, etc. can be produced. It follows that detailed understanding of the *kinetics* of phase transformations in metals and alloys is becoming of overriding importance in a coordinated search for alloys having improved and novel properties.

This work represents an attempt to model the decomposition of austenite to allotriomorphic ferrite, so the part of the time–temperature–transformation (TTT) diagram that is due to this reaction product can be estimated as a function of temperature and alloy chemistry. Emphasis is placed on performing this for multicomponent alloys, because it is these that are relevant both practically and commercially.

Since it is the phase diagram that governs the extent of austenite decomposition, and because austenite and ferrite are to be assumed to be in local equilibrium at the interface, the work described here is heavily dependent upon a suitable thermodynamic model for the iron rich corner of the phase diagram. The model that was employed is described in the Appendix and, in much greater detail, in Ref. 3.

Concept of local equilibrium

The starting assumption for the kinetic analyses of many phase transformations is that of local equilibrium at the moving interface. For the decomposition of austenite to allotriomorphic ferrite in a binary Fe–C steel, local equilibrium implies that the interface adopts the carbon compositions $x_1^{\gamma\alpha}$ and $x_1^{\alpha\gamma}$ in the austenite and ferrite phases respectively, given by the binary phase diagram.[4–6] It also implies that solute and solvent atoms both have atomic mobility outside the interface, because austenite and ferrite have different densities, and therefore mass flow is necessary if the transformation is to be stress free.[5,6] There must exist sufficient atomic mobility within the interface for the reconstruction of the parent lattices to occur there; such mobility destroys any atomic correspondence between the parent and product lattices. The tieline fixing the interface composition passes through the mean alloy composition and the rate of migration of the interface is given by solving Fick's laws, taking conservation of solute into account. In this sense, the kinetic theory is *decoupled* from the thermodynamic theory, because the calculation of the interfacial velocity follows from the unique tieline available.

In a ternary system Fe–C–X, where X represents a substitutional solute, it is in general impossible for the system to choose the tieline passing through the mean alloy composition,[7–12] because of the need to satisfy simultaneously the mass conservation conditions for solute species having very different mobilities: the diffusivities of carbon and X differ typically by six orders of magnitude. The particular tieline chosen depends upon the kinetic theory, so that, in this case, the thermodynamics and kinetics are more strongly *coupled*.

Quantitative theory[7–12] has been developed previously for the prediction of the tieline choice under the local equilibrium assumption. The theory predicts that, at low supersaturations, there is bulk partitioning of the substitutional X, and the activity gradient of carbon in austenite

ahead of the interface is almost zero, so that the necessity for diffusion of carbon away from the α/γ interface is almost entirely eliminated. This is termed the partitioning local equilibrium (or PLE) mode, in recognition of the fact that X partitions during growth.

At high supersaturations, there is negligible partitioning of substitutional solute and a sharp concentration gradient or 'spike' of X exists ahead of the interface; this allows the substitutional solute to keep pace with the carbon. This is termed the negligible partitioning local equilibrium (or NPLE) mode of growth.

Only a small amount of work has been carried out on the kinetic analysis of multicomponent steels. In a recent review, DeHoff[13] showed how the quantitative theory could be applied in this case. However, the cross-terms in the diffusivity matrix were assumed to be negligible, and calculations were not performed. In the present work, the effect of the distribution of substitutional solutes on the flux of carbon ahead of the interface is considered and detailed calculations are performed.

Although the concept of local equilibrium has not yet been tested in a direct sense, i.e. by measurement of the atomic concentrations at and near the interface between two phases, the theory is in broad agreement with diffusion couple experiments,[8] measurements of the growth velocities of individual allotriomorphs,[14] and studies on the bulk partitioning of substitutional solutes as detected using electron microprobes.[15] However, as is discussed below, there are some problems associated with the assumption of local equilibrium at the moving interface; the concept of *paraequilibrium* is often envisaged at high undercoolings. In the following section, the kinetic theory necessary for the prediction of tielines governing interfacial compositions during diffusion controlled growth in ternary Fe–C–X systems is reviewed, then the theory is extended to multicomponent steels.

Growth kinetics

TERNARY Fe–C–X SYSTEM

Kirkaldy[7] was the first to obtain general solutions to the multicomponent diffusion equations for planar, cylindrical, and spherical precipitates. These equations have been applied[8–12] to the ternary system Fe–C–X and a reasonable level of agreement between theory and experiment has been found.

For the ternary system 0–1–2, in which 0 is the solvent (Fe), 1 is an interstitial solute (C), and 2 is a substitutional solute (X) the appropriate diffusion equations for planar growth are[8,9]

$$\frac{\partial c_1}{\partial t} = D_{11}\frac{\partial^2 c_1}{\partial z^2} + D_{12}\frac{\partial^2 c_2}{\partial z^2} \quad \ldots\ldots\ldots (1)$$

and

$$\frac{\partial c_2}{\partial t} = D_{21}\frac{\partial^2 c_1}{\partial z^2} + D_{22}\frac{\partial^2 c_2}{\partial z^2} \quad \ldots\ldots\ldots (2)$$

where D_{ij} are the chemical diffusion coefficients (assumed concentration independent), the c_j are the concentrations in moles per unit volume, z is the coordinate normal to the interface, along which ferrite is growing, and t refers to the time measured from the start of precipitate growth.

Because components 1 and 2 diffuse interstitially and by a vacancy mechanism respectively, it follows that

$$D_{11} \gg D_{22} \quad \ldots\ldots\ldots\ldots\ldots (3)$$

moreover, for dilute solutions, it has been demonstrated[16,17] that

$$D_{11} \gg D_{12} \quad \text{and} \quad D_{22} \gg D_{21} \quad \ldots\ldots\ldots (4)$$

The above conditions indicate that equations (1) and (2) can be approximated by

$$\frac{\partial c_1}{\partial t} = D_{11}\frac{\partial^2 c_1}{\partial z^2} + D_{12}\frac{\partial^2 c_2}{\partial z^2} \quad \ldots\ldots\ldots (5)$$

and

$$\frac{\partial c_2}{\partial t} = D_{22}\frac{\partial^2 c_2}{\partial z^2} \quad \ldots\ldots\ldots\ldots (6)$$

so that the distribution of carbon in austenite can be assumed to have a negligible effect on the flux of X ahead of the α/γ interface.

Coates[9,10] has obtained the solutions to equations (5) and (6) corresponding to the diffusion controlled growth of ferrite, by setting $D_{21} = 0$ in Kirkaldy's general solutions[7] for the ternary system. The solutions can be written

$$c_1 = \bar{c}_1 + \left[\frac{D_{12}(c_2^{\gamma\alpha} - \bar{c}_2)}{D_{11} - D_{22}} + c_1^{\gamma\alpha} - \bar{c}_1\right]\frac{\operatorname{erfc}\{z/2(D_{11}t)^{1/2}\}}{\operatorname{erfc}\{\alpha_1/2(D_{11})^{1/2}\}} - \left[\frac{D_{12}(c_2^{\gamma\alpha} - \bar{c}_2)}{D_{11} - D_{22}}\right]\frac{\operatorname{erfc}\{z/2(D_{22}t)^{1/2}\}}{\operatorname{erfc}\{\alpha_1/2(D_{22})^{1/2}\}} \quad \ldots\ldots (7)$$

$$c_2 = \bar{c}_2 + (c_2^{\gamma\alpha} - \bar{c}_2)\frac{\operatorname{erfc}\{z/2(D_{22}t)^{1/2}\}}{\operatorname{erfc}\{\alpha_1/2(D_{22})^{1/2}\}} \quad \ldots\ldots (8)$$

where $\bar{c}_i$ and $c_i^{\gamma\alpha}$ are the concentrations of component i in the alloy or bulk austenite and in the austenite at the austenite/ferrite interface, respectively. The position of the interface $z = Z$ is given by

$$Z = \alpha_1 t^{1/2} \quad \ldots\ldots\ldots\ldots (9)$$

where α_1 is known as the one-dimensional parabolic rate constant or parabolic thickening constant.

The interfacial mass conservation conditions for components 1 and 2 are respectively

$$(c_1^{\alpha\gamma} - c_1^{\gamma\alpha})\frac{\alpha_1}{2\sqrt{t}} = D_{11}\left.\frac{\partial c_1}{\partial z}\right|_{z=Z} + D_{12}\left.\frac{\partial c_2}{\partial z}\right|_{z=Z} \quad \ldots (10)$$

and

$$(c_2^{\alpha\gamma} - c_2^{\gamma\alpha})\frac{\alpha_1}{2\sqrt{t}} = D_{22}\left.\frac{\partial c_2}{\partial z}\right|_{z=Z} \quad \ldots\ldots\ldots (11)$$

where $c_i^{\alpha\gamma}$ is the concentration of component i in ferrite at the interface. Differentiating equations (7) and (8) with respect to z, combining with equation (9), and substituting into equations (10) and (11) yields

$$f_1 = H_1\{D_{11}\} - \left(\frac{B_1 D_{12}}{D_{11} - D_{22}}\right)(H_1\{D_{22}\} - H_1\{D_{11}\}) \quad \ldots\ldots\ldots (12a)$$

$$f_2 = H_1\{D_{22}\} \quad \ldots\ldots\ldots\ldots (12b)$$

where

$$H_1\{D_{ii}\} = \left(\frac{\pi}{4D_{ii}}\right)^{1/2}\operatorname{erfc}\left\{\frac{\alpha_1}{2D_{ii}^{1/2}}\right\}\exp\left\{\frac{\alpha_1^2}{4D_{ii}}\right\} \quad \ldots (12c)$$

$$B_2 = \frac{c_2^{\gamma\alpha} - c_2^{\alpha\gamma}}{c_1^{\gamma\alpha} - c_1^{\alpha\gamma}} \quad \ldots\ldots\ldots\ldots (12d)$$

and f_1 and f_2 are fractional supersaturations given by

$$f_i = \frac{\bar{c}_i - c_i^{\gamma\alpha}}{c_i^{\alpha\gamma} - c_i^{\gamma\alpha}} \quad \text{for } i = 1, 2 \quad \ldots\ldots\ldots (13)$$

The term B_2 represents the slope of the α/γ interface tieline, provided that on orthogonal ternary isotherms, components 2 and 1 are the ordinate and abscissa, respectively.

Under the assumption of local equilibrium at the interface, only one of $c_1^{\gamma\alpha}$, $c_1^{\alpha\gamma}$, $c_2^{\gamma\alpha}$, and $c_2^{\alpha\gamma}$ is independent, since they are all linked by a tieline of the equilibrium

phase diagram. Equation (12) therefore contains two unknowns and thus can be solved simultaneously to determine the growth velocity and the tieline governing interfacial compositions during growth.

The above theory is based upon the assumption that the diffusion coefficients are concentration independent. While this is probably a reasonable assumption for substitutional elements, the diffusivity of carbon is known to be strongly concentration dependent,[18,19] and in diffusion controlled reactions it is imperative to account for this effect.[5] Trivedi and Pound[20] have demonstrated that for most purposes, a weighted average diffusivity $\bar{D}_{11}$, given by

$$\bar{D}_{11}\{x_1, T\} = \int_{x_1^{\gamma\alpha}}^{\bar{x}_1} \frac{D_{11}\{x_1, T\}}{\bar{x}_1 - x_1^{\gamma\alpha}} \mathrm{d}x_1 \quad \ldots\ldots \quad (14)$$

can adequately represent the effective diffusivity of carbon in austenite. The term x_1 is the mole fraction of carbon in austenite, $x_1^{\gamma\alpha}$ is the mole fraction of carbon in austenite at the interface, and $\bar{x}_1$ is the mole fraction of carbon in austenite remote from the interface. Even though this expression is strictly valid only for steady state growth, Coates[12] has suggested that it should also be a reasonable approximation for parabolic growth. Throughout this work, $\bar{D}_{11}$ is used in place of D_{11}.

Whereas there are many empirical expressions for $D_{11}\{x_1, T\}$, the theoretical representation due to Siller and McLellan[21,22] considers the kinetic and thermodynamic behaviour of carbon in austenite. The model takes into account the concentration dependence of the activity of carbon in austenite and the existence of a finite repulsive interaction between nearest neighbouring carbon atoms situated in octahedral sites.[23] The diffusivity is represented by

$$D_{11}\{x_1, T\} = (kT/h)(\exp\{-\Delta G^*/kT\})(\lambda^2/3\Gamma_m)\eta\{\theta\} \quad \ldots\ldots \quad (15a)$$

where

$$\eta\{\theta\}/a_1^{\gamma} = 1 + \{W(1+\theta)[1 - (0{\cdot}5W + 1)\theta + (0{\cdot}25W^2 + 0{\cdot}5W)(1-\phi)\theta^2]\} + (1/a_1^{\gamma})(1+\theta)(\partial a_1^{\gamma}/\partial\theta) \quad \ldots\ldots \quad (15b)$$

where k and h are the Boltzmann and Planck constants respectively, W is the number of octahedral interstices around a single such interstice (equal to 12 in austenite), ΔG^* is an activation free energy, Γ_m is an activity coefficient, λ is the distance between {002} austenite planes, and a_1^{γ} is the activity of carbon in austenite. The term ϕ is given by $\phi = 1 - \exp\{-\omega_{\gamma}/kT\}$, where ω_{γ} is the nearest neighbour carbon–carbon interaction energy (taken to be 8250 J mol^{-1}) and θ is the ratio of the number of carbon atoms to the total number of solvent atoms, given by $\theta = x_1/(1-x_1)$. Bhadeshia[25] found $\Delta G^*/k = 21\,230$ K and $\ln\{\Gamma_m/\lambda^2\} = 31{\cdot}84$. Substitutional alloying elements change the carbon–carbon interaction energy ω_{γ}, and therefore influence D_{11}. The method adopted here to account for this effect follows that due to Bhadeshia.[26]

The on-diagonal diffusion coefficients D_{ii} for substitutional elements can be evaluated from the compilation due to Fridberg and co-workers.[27] Provided the solution is dilute, the cross-terms D_{1i} can be expressed[16] in terms of the Wagner interaction parameters ε_{ij}

$$D_{1i}/D_{11} = \frac{\varepsilon_{1i}x_1}{1 + \varepsilon_{11}x_1} \quad \ldots\ldots \quad (16)$$

The ratio D_{1i}/D_{11} is also concentration dependent, but numerical calculations[28] suggest that the use of a constant D_{1i}/D_{11}, evaluated at the interfacial composition $x_1^{\gamma\alpha}$, gives an adequate approximation to the problem.[12]

EXTENSION TO MULTICOMPONENT SYSTEM

The kinetic theory developed by Kirkaldy, Coates, and other workers applies to ternary systems of the form Fe–C–X and testing of the theory has always been carried out against 'model' ternary alloys. There is obviously a great desire to develop such kinetic theory for multicomponent steels, because it is these that are important both practically and commercially. The above analysis is now extended to multicomponent steels, in which a number of substitutional components have been added to the Fe–C binary.

To do this, it is necessary to adopt further assumptions, which make the problem of tieline choice easier. In the following analysis, it is implicit that substitutional–substitutional terms D_{jk} $(j, k > 1)$ in the diffusivity matrix are negligible. This amounts to the assumption that the flux of one substitutional element is not influenced by the presence of a (possibly large) concentration gradient of a second. Although this may be a major assumption, in many cases experimental measurements of the cross-terms in the diffusivity matrix have not been carried out.

By analogy with equations (5) and (6), the multicomponent diffusion equations considered here are

$$\frac{\partial c_1}{\partial t} = \sum_{i=1}^{n} D_{1i}\frac{\partial^2 c_i}{\partial z^2} \quad \ldots\ldots \quad (17)$$

and

$$\frac{\partial c_i}{\partial t} = D_{ii}\frac{\partial^2 c_i}{\partial z^2} \quad \text{for } i = 2 \rightarrow n \quad \ldots\ldots \quad (18)$$

It is possible to demonstrate by substitution that the solutions to equations (17) and (18) are

$$c_1 = \bar{c}_1 + \left\{\sum_{i=2}^{n}\left[\frac{D_{1i}(c_i^{\gamma\alpha} - \bar{c}_i)}{D_{11} - D_{ii}}\right] + c_1^{\gamma\alpha} - \bar{c}_1\right\} \times \frac{\mathrm{erfc}\{z/2(D_{11}t)^{1/2}\}}{\mathrm{erfc}\{\alpha_1/2(D_{11})^{1/2}\}} - \sum_{i=2}^{n}\left[\frac{D_{1i}(c_i^{\gamma\alpha} - \bar{c}_i)}{D_{11} - D_{ii}}\right]\frac{\mathrm{erfc}\{z/2(D_{ii}t)^{1/2}\}}{\mathrm{erfc}\{\alpha_1/2(D_{ii})^{1/2}\}} \quad \ldots \quad (19)$$

and

$$c_i = \bar{c}_i + (c_i^{\gamma\alpha} - \bar{c}_i)\frac{\mathrm{erfc}\{z/2(D_{ii}t)^{1/2}\}}{\mathrm{erfc}\{\alpha_1/2(D_{ii})^{1/2}\}} \quad \text{for } i = 2 \rightarrow n \quad (20)$$

The mass conservation conditions are now

$$(c_1^{\alpha\gamma} - c_1^{\gamma\alpha})\frac{\alpha_1}{2\sqrt{t}} = D_{11}\left.\frac{\partial c_1}{\partial z}\right|_{z=Z} + \sum_{i=2}^{n} D_{1i}\left.\frac{\partial c_i}{\partial z}\right|_{z=Z} \quad \ldots \quad (21)$$

and

$$(c_i^{\alpha\gamma} - c_i^{\gamma\alpha})\frac{\alpha_1}{2\sqrt{t}} = D_{ii}\left.\frac{\partial c_i}{\partial z}\right|_{z=Z} \quad \text{for } i = 2 \rightarrow n \quad \ldots \quad (22)$$

where $c_i^{\alpha\gamma}$ is the concentration of component i in ferrite. By differentiating equations (19) and (20) with respect to z, combining with equation (9), and substituting into equations (21) and (22), the problem of tieline choice can be expressed by

$$f_1 = H_1\{D_{11}\} - \sum_{i=2}^{n}\left(\frac{B_i D_{1i}}{D_{11} - D_{ii}}\right)(H_1\{D_{ii}\} - H_1\{D_{11}\}) \quad \ldots\ldots \quad (23a)$$

$$f_i = H_1\{D_{ii}\} \quad \text{for } i = 2 \rightarrow n \quad \ldots\ldots \quad (23b)$$

where

$$H_1\{D_{ii}\} = \left(\frac{\pi}{4D_{ii}}\right)^{1/2}\mathrm{erfc}\left\{\frac{\alpha_1}{2D_{ii}^{1/2}}\right\}\exp\left\{\frac{\alpha_1^2}{4D_{ii}}\right\} \quad \ldots \quad (23c)$$

$$B_i = \frac{c_i^{\gamma\alpha} - c_i^{\alpha\gamma}}{c_1^{\gamma\alpha} - c_1^{\alpha\gamma}} \quad \text{for } i = 2 \rightarrow n \quad \ldots\ldots \quad (23d)$$

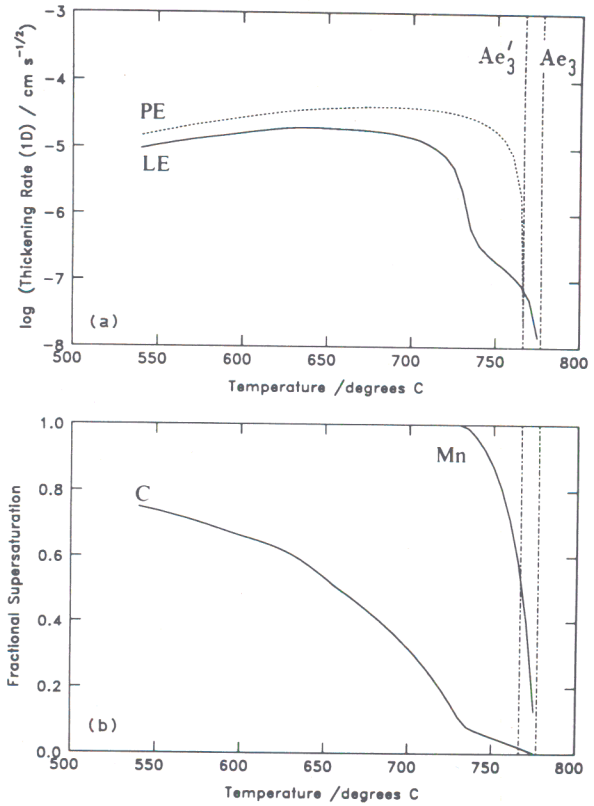

a one-dimensional thickening constant α_1 evaluated under local equilibrium (LE) and paraequilibrium (PE) assumptions as function of temperature; *b* associated fractional supersaturations

1 Fe–0·33C–1·00Mn (wt-%) ternary alloy

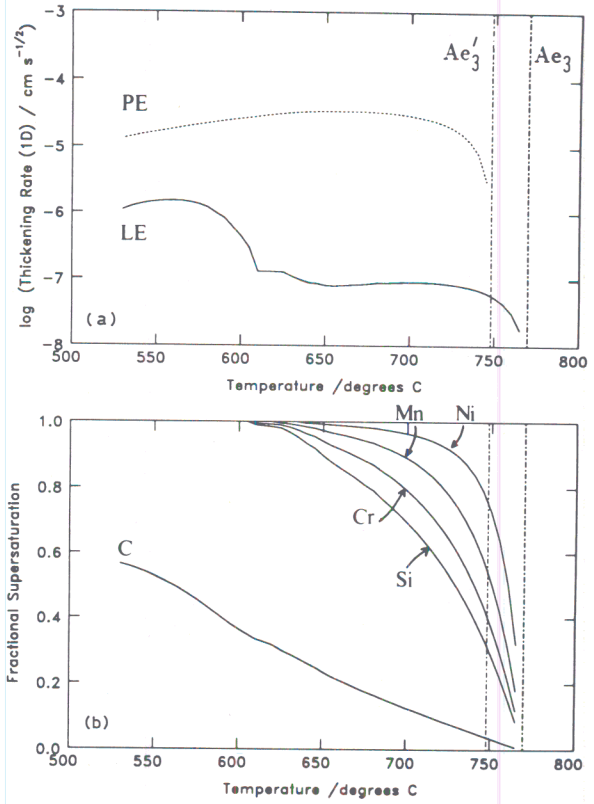

a one-dimensional thickening constant α_1 evaluated under local equilibrium (LE) and paraequilibrium (PE) assumptions as function of temperature; *b* associated fractional supersaturations

2 Multicomponent En 16 steel

In all the calculations that follow, the terms D_{1i} are evaluated according to equation (16). Although this equation was derived[16,17] for the ternary system, the assumptions implicit in writing equation (18) mean that no further assumptions are introduced if this equation is adopted.

PARAEQUILIBRIUM

There are some problems associated with the above theory. With decreasing temperature, the local equilibrium assumption predicts[9] that the width of the solute 'spike' rapidly approaches the width of the interface itself. Even before the concentration gradient reaches such an unfeasible magnitude, it is not clear whether the substitutional atoms possess the atomic mobility necessary to partition ahead of the interface.

The concept of *paraequilibrium* has been introduced[29–31] to describe the kinetically constrained equilibrium in which, subject to the constraint that substitutional alloying elements do not redistribute during transformation, the carbon atoms at the interface are in local equilibrium. In this case, it is then implicit that the chemical potentials of iron and the substitutional elements change abruptly at the α/γ interface.

Under the assumption of paraequilibrium, there is only one possible tieline for the interface to choose at constant temperature, because the ratio of the concentration of iron to that of each of the substitutionals is constant. It is therefore necessary to determine only $c_1^{\gamma\alpha}$ and $c_1^{\alpha\gamma}$ as functions of temperature. In this case, the kinetic theory is once again decoupled from the thermodynamic theory; the one-dimensional parabolic thickening rate can then be determined from the equation

$$f_1 = H_1\{\bar{D}_{11}\} \quad \ldots\ldots\ldots\ldots\ldots\ldots \quad (24)$$

where $\bar{D}_{11}$ is the weighted average diffusivity, given by equation (14).

Finally, it should be noted that the lack of bulk partitioning of substitutional alloying elements is insufficient to distinguish between the NPLE and the paraequilibrium modes of transformation; the substitutional alloying composition in austenite must be measured at the α/γ interface. In addition, as will be seen in the calculations that follow, the difference between the interfacial velocities calculated under the local equilibrium and paraequilibrium modes becomes very small at high undercoolings.

Calculation of parabolic thickening rate

If the $\alpha/(\alpha+\gamma)$ and $\gamma/(\gamma+\alpha)$ surfaces are known as functions of alloy chemistry, the above equations can be solved to yield a value for the one-dimensional thickening constant α_1 for the multicomponent system. It is therefore necessary to couple the thermodynamic model to the kinetic model, because the multicomponent tielines need to be known. The calculations must necessarily involve iterative processes, since the equations are non-linear. In the following calculations, one further assumption is made that

$$f_i = \frac{\bar{c}_i - c_i^{\gamma\alpha}}{c_i^{\alpha\gamma} - c_i^{\gamma\alpha}} \approx \frac{\bar{x}_i - x_i^{\gamma\alpha}}{x_i^{\alpha\gamma} - x_i^{\gamma\alpha}} \quad \text{for } i = 1 \to n \quad \ldots\ldots \quad (25)$$

so that the supersaturations in equations (23) and (24) are calculated using concentrations expressed as mole fractions. This is equivalent to the assumption that the densities of austenite and ferrite are equal.

To illustrate the behaviour predicted by the theory, calculations have been carried out on three alloys, namely, a ternary alloy Fe–0·33C–1·00Mn (wt-%), as well as En 16 and En 19,[32] the last two being multicomponent steels. The rate constants calculated under the local equilibrium, and paraequilibrium assumptions, are presented in Figs. 1,

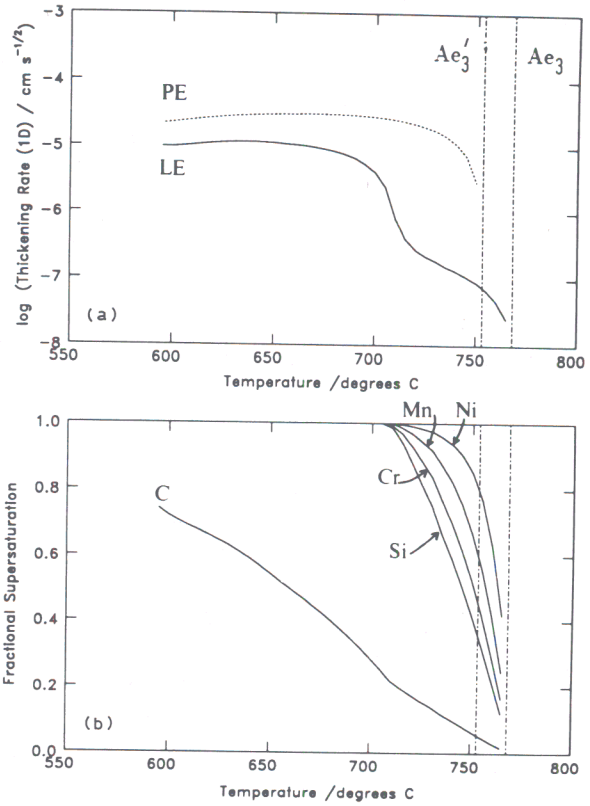

a one-dimensional thickening constant α_1 evaluated under local equilibrium (LE) and paraequilibrium (PE) assumptions as function of temperature; *b* associated fractional supersaturations

3 Multicomponent En 19 steel

2, and 3 respectively, together with the values of the supersaturations, as given by equation (13).

The predicted behaviour can be summarised as follows. Under PLE, the supersaturations of the substitutional solutes increase with decreasing temperature, finally becoming very nearly equal to unity on entry into the NPLE regime; at this temperature, α_1 increases dramatically. At lower temperatures, α_1 decreases in magnitude, reflecting the decreasing diffusivities. At temperatures below Ae'_3, α_1 calculated under the paraequilibrium assumption is greater than that calculated under local equilibrium. However, at temperatures within the NPLE regime, the difference is only marginal. This effect occurs because, at low temperatures, the substitutional–substitutional diffusional interaction has little influence on the growth kinetics, because the carbon distribution becomes too steep to respond to the X distribution.[10] In this case, equation (23*a*) reduces to

$$f_1 = H_1\{D_{11}\} - \sum_{i=2}^{n}\left(\frac{B_i D_{1i}}{D_{11}-D_{ii}}\right)(H_1\{D_{ii}\} - H_1\{D_{11}\})$$
$$\approx H_1\{D_{11}\} \quad \ldots\ldots\ldots\ldots \quad (26)$$

The results are in qualitative agreement with the recent calculations of Enomoto,[33] although this analysis was limited to ternary systems.

Nucleation and growth theory

Recently, Bhadeshia *et al.*[34] described theory capable of modelling the nucleation and growth of allotriomorphic ferrite. The allotriomorphs, before site saturation, are modelled as discs having their faces parallel to the austenite

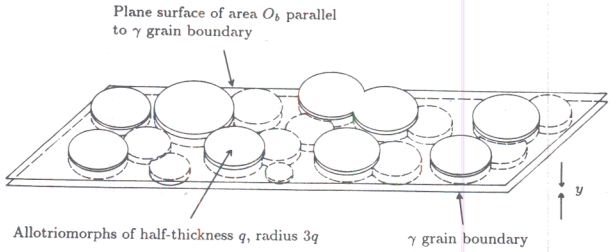

4 Model for nucleation and growth of allotriomorphic ferrite: allotriomorphs are modelled as discs of half-thickness q and radius $3q$ such that their faces lie parallel to austenite grain boundary

grain boundary plane (Fig. 4). The discs are assumed to grow radially, with the half-thickness q and radius ηq varying parabolically with time, through the equation $q = \alpha_1 t^{1/2}$. The aspect ratio η of the allotriomorphs is considered constant, because the lengthening and thickening processes are actually coupled; consistent with the experimental evidence,[35] η is taken as 3·0.

The approach closely follows Cahn's analysis[36] of grain boundary nucleation and growth kinetics and is as follows. Consider a plane surface of total area O_b parallel to a particular boundary; the extended area O_α^{ex} is defined as the sum of the areas of intersection of the discs with this plane. It follows that the small change δO_α^{ex} in O_α^{ex} due to a disc nucleated between $t = \tau$ and $t = \tau + \delta\tau$ is

$$\delta O_\alpha^{ex} = \tau O_b I_B[(\eta\alpha_1)^2(t-\tau)]\delta\tau \quad \text{if } \alpha_1(t-\tau)^{1/2} > y \quad \ldots\ldots\ldots \quad (27a)$$

and

$$\delta O_\alpha^{ex} = 0 \quad \text{if } \alpha_1(t-\tau)^{1/2} < y \quad \ldots\ldots\ldots \quad (27b)$$

where I_B is the grain boundary steady state nucleation rate per unit area of boundary. The term τ is the incubation time for the nucleation of one particle. Only allotriomorphs nucleated for $\tau > (y/\alpha_1)^2$ can contribute to the extended area intersected by the plane at y; if τ takes a value less than $(y/\alpha_1)^2$, then the allotriomorph has not had sufficient time to grow the distance y to the arbitrary plane. It follows that the entire extended area is given by

$$O_\alpha^{ex} = \int_0^{t-(y/\alpha_1)^2} (\eta\alpha_1)^2 \pi O_b I_B (t-\tau)\, d\tau$$
$$= \tfrac{1}{2}\pi O_b I_B (\eta\alpha_1)^2 t^2 (1-\theta^4) \quad \ldots\ldots\ldots \quad (28)$$

where $\theta = y/(\alpha_1 t^{1/2})$, corresponding to the ratio between the distance to the arbitrary plane and the half-thickness of the allotriomorph at time t.

The actual area O_α which intersects the plane O_b will be somewhat smaller than the extended area, because the extended area includes a fraction $[1-(O_\alpha/O_b)]$ of 'phantom' area which has already transformed to ferrite. The relationship between the extended area and the actual area O_α is then given by[36,37]

$$O_\alpha^{ex}/O_b = \ln\{1-(O_\alpha/O_b)\} \quad \ldots\ldots\ldots \quad (29)$$

Assuming that there is no interference with allotriomorphs from other boundaries, the total volume V_b of material originating from this grain boundary is given by integrating y between negative and positive infinity; in terms of θ this gives

$$V_b = 2\int_0^1 O_b \alpha_1 t^{1/2}(1-\exp\{-O_\alpha^{ex}/O_b\})\, d\theta$$
$$= 2\int_0^1 O_b \alpha_1 t^{1/2}[1-\exp\{-0{\cdot}5\pi I_B(\eta\alpha_1)^2 t^2(1-\theta^4)\}]\, d\theta$$
$$= 2O_b\alpha_1 t^{1/2} f\{\eta\alpha_1, I_B, t\} \quad \ldots\ldots\ldots \quad (30)$$

where

$$f\{\eta\alpha_1, I_B, t\} = \int_0^1 1 - \exp\{-0{\cdot}5\pi I_B(\eta\alpha_1)^2 t^2(1-\theta^4)\}\,d\theta \quad \ldots\ldots\ldots (31)$$

If the total grain boundary area is $O_B = \Sigma O_b$, then, by substituting O_B for O_b in the above equation, the total extended volume V_α^{ex} of material is found; this is an extended volume, because allowance was not made for impingement of discs originating from different boundaries. Thus,

$$V_\alpha^{ex} = 2O_B\alpha_1 t^{1/2} f\{\eta\alpha_1, I_B, t\} \quad \ldots\ldots\ldots (32)$$

and if V is the total volume, and S_V the γ grain surface area per unit volume, then

$$V_\alpha^{ex}/V = 2S_V\alpha_1 t^{1/2} f\{\eta\alpha_1, I_B, t\} \quad \ldots\ldots\ldots (33)$$

This can be converted into the actual volume V_α using the following equation (related to equation (29))

$$V_\alpha/(V\phi) = 1 - \exp\{-V_\alpha^{ex}/(V\phi)\} \quad \ldots\ldots\ldots (34)$$

where ϕ is the equilibrium volume fraction of ferrite, so that $V\phi$ is the volume of ferrite in the austenite matrix. The term ϕ can be estimated from the phase diagram, by calculation of the tieline passing through the mean alloy composition

$$\phi = \frac{\bar{c}_i - c_i^{\gamma\alpha}}{c_i^{\alpha\gamma} - c_i^{\gamma\alpha}} \quad \ldots\ldots\ldots\ldots\ldots (35)$$

Since the tieline under consideration passes through the overall alloy composition, ϕ can be evaluated using the c values of any of the components in the system. It should be noted that in the paraequilibrium mode of transformation, ϕ is equal to f_1, independent of the volume fraction transformed. Under local equilibrium, ϕ does not equal any of the values f_i until the end of the transformation, when austenite and ferrite reach their equilibrium volume fractions.

It follows that

$$-\ln\{1-\zeta\} = 2(S_V/\phi)\alpha_1 t^{1/2} f\{\eta\alpha_1, I_B, t\} \quad \ldots\ldots (36)$$

where $\zeta = V_\alpha/(V\phi)$ is often referred to as the extent of reaction. It corresponds to the volume of α divided by its equilibrium volume.

The value of the integral f tends to unity as I_B increases or time increases, since site saturation occurs. In the limit, as the integral tends to unity, equation (36) simplifies to one-dimensional thickening governed by the equation

$$-\ln\{1-\zeta\} = 2(S_V/\phi)\alpha_1 t^{1/2} \quad \ldots\ldots\ldots (37)$$

In summary, the theory takes into account hard impingement between allotriomorphs growing from the same, or adjacent, austenite grain boundaries. It should be noted, however, that soft impingement (the overlap of diffusion fields) between neighbouring allotriomorphs is ignored.

Classical nucleation theory

To use the above theory to estimate the time–temperature–transformation (TTT) curves for the decomposition of austenite to allotriomorphic ferrite, it is necessary to derive a function that describes the process of nucleation. Following classical nucleation theory (e.g. Ref. 6), the steady state rate of nucleation on grain boundary faces per unit area of boundary is given by

$$I_B^f = N^f \frac{kT}{h} \exp\left\{\frac{-(\Delta G_{crit}^f + Q)}{kT}\right\} \quad \ldots\ldots\ldots (38)$$

where N^f is the number of face sites per unit area of boundary supporting nucleation, k is the Boltzmann constant, h is the Planck constant, T is the absolute temperature, ΔG_{crit}^f is the critical activation free energy per atom for nucleation on faces, and Q is an activation free energy per atom, for atoms crossing the austenite/ferrite nucleus interface. The term kT/h is in effect a frequency factor for atomic vibrations in the crystal lattice.

In the calculations that follow, N^f is defined through the equation

$$N^f = K_1^f/a^2 \quad \ldots\ldots\ldots\ldots\ldots (39)$$

where K_1^f is the fraction of face sites supporting nucleation and a is the interatomic spacing, taken as 0·25 nm. The term K_1^f allows for the 'poisoning' of possible nucleation sites on the boundary.

There are many expressions available for the critical activation energy ΔG_{crit}^f. If the strain energy associated with the nucleus is ignored, common expressions are of the form (e.g. Refs. 38, 39)

$$\Delta G_{crit}^f = \frac{\sigma^3}{\Delta G_V^2} K_2^f \quad \ldots\ldots\ldots\ldots\ldots (40)$$

where ΔG_V is the free energy per unit volume for ferrite nucleation from supersaturated austenite (calculated here using the parallel tangent construction) and σ is the austenite/ferrite nucleus interfacial energy per unit area, which is taken as 0·2 J m^{-2}, which is assumed not to vary with interfacial orientation or alloy chemistry. The multiplication factor K_2^f takes into account non-spherical nucleus shape (e.g. Ref. 39).

Nucleation is also possible on grain boundary edges and corners, where different site densities and activation energies apply. For nucleation on edges, the following expression is adopted for the rate of nucleation on grain boundary edges per unit area of boundary I_B^e

$$I_B^e = \frac{N^e}{a}\frac{kT}{h} \exp\left\{\frac{-(\Delta G_{crit}^e + Q)}{kT}\right\} \quad \ldots\ldots\ldots (41)$$

where N^e is the number of edge sites per unit edge of boundary supporting nucleation and ΔG_{crit}^e is the critical activation free energy per atom for nucleation on grain edges. The term N^e is defined through the equation

$$N^e = \frac{K_1^e}{a} \quad \ldots\ldots\ldots\ldots\ldots (42)$$

where K_1^e is the fraction of edge sites supporting nucleation and ΔG_{crit}^e is given by

$$\Delta G_{crit}^e = \frac{\sigma^3}{\Delta G_V^2} K_2^e \quad \ldots\ldots\ldots\ldots\ldots (43)$$

where K_2^e is a constant taking into account the shape of the critical nucleus.

For nucleation on corners, the expressions considered are as follows

$$I_B^c = \frac{N^c}{a^2}\frac{kT}{h} \exp\left\{\frac{-(\Delta G_{crit}^c + Q)}{kT}\right\} \quad \ldots\ldots\ldots (44)$$

where I_B^c is the rate of nucleation on grain boundary corners per unit area of boundary and $N^c = K_1^c$ represents the fraction of corner sites supporting nucleation. The term ΔG_{crit}^c is given by

$$\Delta G_{crit}^c = \frac{\sigma^3}{\Delta G_V^2} K_2^c \quad \ldots\ldots\ldots\ldots\ldots (45)$$

where K_2^c is the shape factor for corner nucleation.

Summing the contributions from faces, edges, and corners, the total nucleation rate (to be used in equation (36)) is given by the expression

$$I_B = I_B^f + I_B^e + I_B^c \quad \ldots\ldots\ldots\ldots\ldots (46)$$

As discussed by Cahn[36] and Christian[6] the order

$K_2^f > K_2^e > K_2^c$ is expected, so that $\Delta G^f_{crit} > \Delta G^e_{crit} > \Delta G^c_{crit}$. However, the relative nucleation rates do not necessarily increase in the same order as the activation energies for nucleation decrease,[6] since the density of sites also decreases as the mode of nucleation changes from faces, to edges, and finally to grain boundary corners. It is to be expected that $N^f > N^e/a > N^c/a^2$. This means that, with decreasing temperature, corners, edges, and finally faces make the greatest contribution to the nucleation rate.

It is possible to make approximations to equations (38), (41), and (44). For example, at temperatures well below the Ae_3, nucleation at faces is likely to dominate; moreover, the activation free energy for nucleation becomes relatively small and the diffusion of atoms across the austenite/ferrite nucleus is the rate controlling step; equation (38) then approximates to

$$I_B^f \approx N^f \frac{kT}{h} \exp\left\{\frac{-Q}{kT}\right\} \quad \ldots\ldots\ldots\ldots \quad (47)$$

At slightly higher temperatures, nucleation is dominated by a high ΔG^f_{crit}, which is in turn dependent upon the driving force for transformation and the interfacial energy; equation (38) then approximates to

$$I_B^f \approx N^f \frac{kT}{h} \exp\left\{\frac{-\Delta G^f_{crit}}{kT}\right\} \quad \ldots\ldots\ldots\ldots \quad (48)$$

Method of fit to experimental data

The experimental data chosen for analysis are contained in the BISRA atlas,[32] which is one of the more meticulously determined sets of TTT curves. Since it is necessary to distinguish between the parts of the C-curves representing the formation of allotriomorphic ferrite due to reconstructive diffusion or displacive reactions (such as Widmanstätten ferrite of bainite), only those diagrams having readily distinguishable component curves were used in the following analysis. The analysis is also restricted to steels that are sufficiently dilute for the thermodynamic model to be applicable; following Kirkaldy and Baganis[40] the total substitutional alloying content of the steels analysed is less than 6 wt-%. The steels selected, together with the chemical compositions and ASTM grain size numbers are given in Table 1. Also tabulated are the Ae_3 and Ae'_3 temperatures calculated using the thermodynamic model.

The term S_V required in equation (36) has been calculated from the ASTM grain size numbers presented in the BISRA atlas using the following equation[41]

$$S_V = 2000 \times 10^{(ASTM + 3{\cdot}298)/6{\cdot}6457} \quad \ldots\ldots\ldots \quad (49)$$

Table 1 Chemical compositions, equilibrium (Ae_3) and paraequilibrium (Ae'_3) $(\alpha+\gamma)/\gamma$ boundary temperatures, and ASTM grain size numbers of steels analysed in present work

Steel	Composition, wt-%						Ae_3, °C	Ae'_3, °C	ASTM grain size no.
	C	Si	Mn	Cr	Mo	Ni			
En 13	0·19	0·14	1·37	0·20	0·31	0·56	792	774	7
En 16	0·33	0·18	1·48	0·16	0·27	0·26	770	748	8
En 17	0·38	0·25	1·49	0·14	0·41	0·24	764	740	8
En 18	0·48	0·25	0·86	0·98	0·04	0·18	753	734	5·5
En 19	0·41	0·23	0·67	1·01	0·23	0·20	768	753	8
En 20	0·27	0·13	0·60	0·74	0·55	0·19	796	786	8
En 20	0·41	0·28	0·58	1·39	0·74	0·15	773	757	7·5
En 24	0·38	0·20	0·69	0·95	0·26	1·58	749	725	7
En 100	0·40	0·21	1·34	0·53	0·22	1·03	745	715	6
En 110	0·39	0·23	0·62	1·11	0·18	1·44	751	728	7
En 354	0·19	0·21	0·90	1·08	0·18	1·87	772	746	8
En 355	0·20	0·23	0·61	1·65	0·19	2·00	771	746	8

where ASTM is the ASTM grain size number and S_V (m^{-1}) is the austenite grain boundary area per unit volume.

In principle, the model developed is capable of calculating the experimental C-curves, before the onset of soft impingement. However, the constants K_1^f, K_1^e, K_1^c, K_2^f, K_2^e, K_2^c, and Q remain unknown. The method adopted here involves determining the values of these constants, by fitting against the experimental C-curves. The values chosen could then be regarded as universal constants, which should be applicable to all low alloy steels. In this way it would then be possible to extrapolate with confidence between steels of different compositions.

Thus, the nucleation rate I_B necessary to reproduce the experimentally determined C-curves has been calculated as a function of temperature. Because soft impingement must eventually occur, only the C-curves corresponding to 0, 10, and 50% transformation in the BISRA atlas are considered and, for the purposes of calculation, the 0% curve is taken as corresponding to 0·1% transformation.

From equation (47), a plot of $\ln\{I_B\} - \ln\{kT/h\}$ versus $1/T$ should yield a straight line of gradient Q and intercept N^f at low temperatures. From equations (41), (44), and (48) a plot of $(\ln\{I_B\} - \ln\{kT/h\} + Q)/kT$ versus $1/(T\Delta G_V^2)$ should yield three straight lines, with decreasing intercepts N^f, N^e/a, and N^c/a^2, and decreasing (negative) gradients $\sigma^3 K_2^f/k$, $\sigma^3 K_2^e/k$, and $\sigma^3 K_2^c/k$ as the temperature increases; these lines correspond to the regimes in which face, edge, and finally corner nucleation dominate.

However, as is shown below, the scatter associated with the experimental data means that it is difficult to determine the boundaries between the regimes with precision. After some trial and error, the ranges of application for the equilibrium and paraequilibrium mechanisms were decided and are presented here in Table 2.

Results

Figures 5 and 6 (for equilibrium and paraequilibrium respectively) illustrate the extent to which the data fall on straight lines. Linear regression analysis was used to determine the best-fit lines through the data points; from these lines the constants necessary to define the nucleation function were calculated. The values are given in Tables 3 and 4 together with errors based upon the standard errors in the gradients and intercepts of the best-fit lines in the figures. The values of Q determined correspond to 800 kJ mol^{-1} (equilibrium) and 350 kJ mol^{-1} (paraequilibrium). It seems intuitively reasonable to expect that Q should be comparable to the activation energy for self-diffusion in iron, which is close to 250 kJ mol^{-1} (Ref. 27).

Table 2 Equations and corresponding ranges of application for equilibrium and paraequilibrium mechanisms

Equation no.	Range of application
Equilibrium	
(47)	$T < 640$°C
(48)	$1/(T\Delta G_V^2) < 2 \times 10^{-18}$ K^{-1} (J $atom^{-1})^{-2}$
(41)	2×10^{-18} K^{-1} (J $atom^{-1})^{-2} < 1/T\Delta G_V^2 < 6{\cdot}75 \times 10^{-18}$ K^{-1} (J $atom^{-1})^{-2}$
(44)	$1/T\Delta G_V^2 > 6{\cdot}75 \times 10^{-18}$ K^{-1} (J $atom^{-1})^{-2}$
Paraequilibrium	
(47)	$T < 640$°C
(48)	$1/T\Delta G_V^2 < 5 \times 10^{-18}$ K^{-1} (J $atom^{-1})^{-2}$
(41)	5×10^{-18} K^{-1} (J $atom^{-1})^{-2} < 1/T\Delta G_V^2 < 3 \times 10^{-17}$ K^{-1} (J $atom^{-1})^{-2}$
(44)	$1/T\Delta G_V^2 > 3 \times 10^{-17}$ K^{-1} (J $atom^{-1})^{-2}$

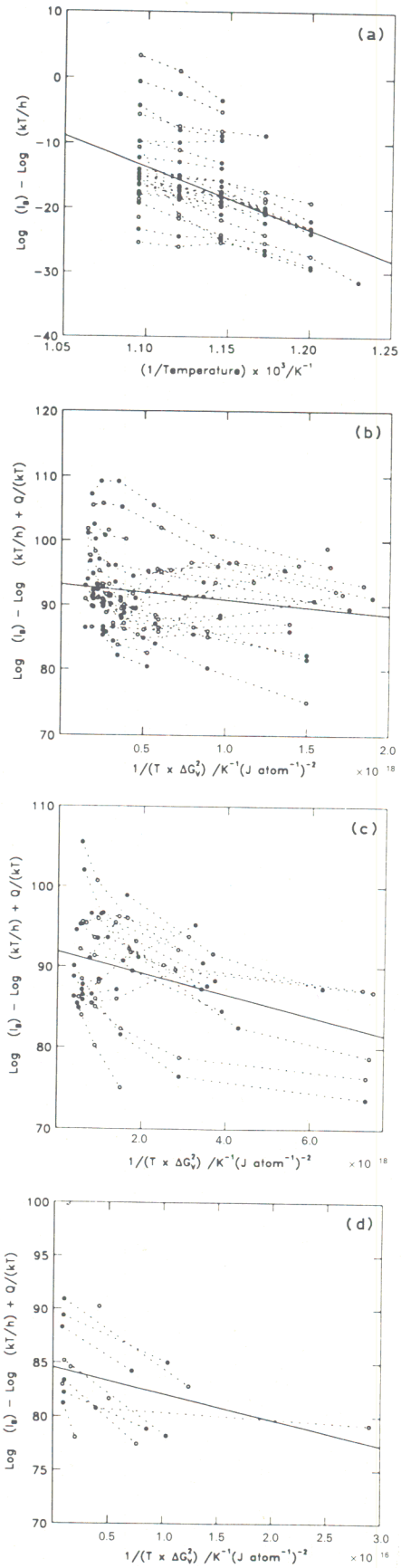

a equation (47); *b* equation (48); *c* equation (41); *d* equation (44)

5 Determination of constants for nucleation assuming equilibrium mode for nucleation and growth

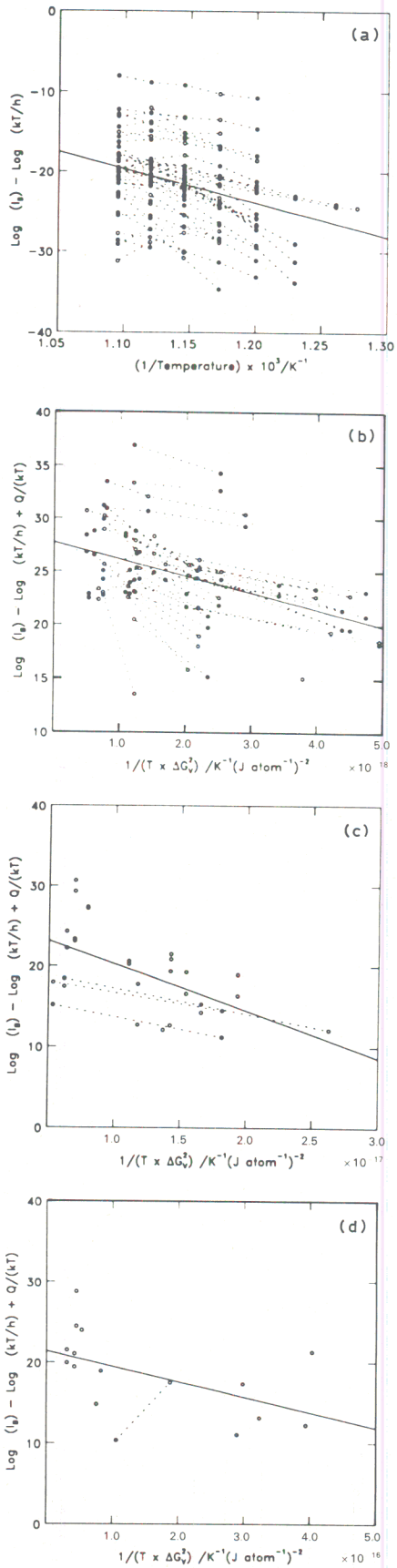

a equation (47); *b* equation (48); *c* equation (41); *d* equation (44)

6 Determination of constants for nucleation assuming paraequilibrium mode for nucleation and growth

Table 3 Values of nucleation constants, assuming nucleation and growth by equilibrium mode of transformation: from Fig. 5*a*, $Q = (1{\cdot}3 \pm 0{\cdot}2) \times 10^{-18}$ J atom^{-1} and value of K_1^f derived from Fig. 5*b* is used throughout rest of work

Fig. no.	Fraction supporting nucleation K_1		Shape factor K_2
	Average	Standard error	
5*a*	$K_1^f = 1 \times 10^{21}$	$K_1^f = 5 \times 10^{12}$–2×10^{29}	...
5*b*	$K_1^f = 1{\cdot}9 \times 10^{21}$	$K_1^f = 7{\cdot}4 \times 10^{20}$–$4{\cdot}4 \times 10^{21}$	$K_2^f = (4{\cdot}0 \pm 2{\cdot}0) \times 10^{-3}$
5*c*	$K_1^e = 4{\cdot}9 \times 10^{20}$	$K_1^e = 1{\cdot}8 \times 10^{20}$–$1{\cdot}3 \times 10^{21}$	$K_2^e = (2{\cdot}3 \pm 0{\cdot}6) \times 10^{-3}$
5*d*	$K_1^c = 3{\cdot}3 \times 10^{17}$	$K_1^c = 1{\cdot}1 \times 10^{17}$–$1{\cdot}0 \times 10^{18}$	$K_2^c = (4{\cdot}2 \pm 2{\cdot}2) \times 10^{-5}$

Figures 7 and 8 illustrate the level of agreement between the experimentally observed C-curves and those calculated using the model developed here.

Discussion

It has been demonstrated that the kinetic model, based upon the general principles of thermodynamic and phase transformation theory, is capable of reproducing the C-curve behaviour exhibited by allotriomorphic ferrite transformation from supersaturated austenite. It could therefore be argued that the general kinetic features of the transformation have been explained. However, there are points which have arisen during this analysis which warrant further discussion.

The constants K_1^f, K_1^e, and K_1^c represent physically the fraction of face, edge, and corner sites supporting nucleation. The maximum value which each can take is then unity, but in practice a somewhat lower value is expected because not all heterogeneous sites are likely to support nucleation. The values of K_1^f, K_1^e, and K_1^c inferred assuming local equilibrium during both nucleation and growth are therefore physically unreasonable (Table 3). In addition, the shapes of the computed C-curves (Fig. 7) reflect the large increase in the interfacial velocity predicted when the temperature falls into the NPLE regime. This is not detected in practice.

On the other hand, the values of K_1^f, K_1^e, and K_1^c inferred assuming paraequilibrium are physically reasonable (Table 4), as are the shapes of the calculated C-curves (Fig. 8). For this reason, this work suggests that, at temperatures only slightly below the Ae'_3, austenite decomposes to allotriomorphic ferrite by paraequilibrium transformation and that this growth mode operates over a large part of the observed range of transformation. However, it should be pointed out that this work does not deny the fact that substitutional element mobility, and thus partition between the parent and product lattices, remains a possibility for some or all of the substitutional components, becoming increasingly likely as the supercooling below Ae_3 decreases. Ultimately, at temperatures between Ae_3 and Ae'_3, any observed growth must occur with partition, this being a thermodynamic necessity.

That the paraequilibrium mode of growth might be dominant has often been suggested (Refs. 29–31), but there is a problem in distinguishing experimentally between the NPLE and paraequilibrium modes of growth. This occurs because both modes imply lack of partition between parent and product phases, so that direct observation[42,43] of lack of partition does not in itself constitute proof that one or other of the modes is operating. (Conversely, direct observation of partition between parent and product phases does imply substitutional element mobility and thus PLE growth.) Thus, arguments concerning whether the NPLE or paraequilibrium mode is operative have hinged upon whether the observed parabolic thickening rates are consistent with values calculated assuming the proposed growth modes.[43–46] One problem is that the methods used for direct measurement of the parabolic thickening rates,[14] although rather ingenious, are subject to experimental complications that lead inevitably to large uncertainties in the reported values. More direct evidence could be gleaned by very fine scale microanalytical techniques having resolution down to atomic level. Energy dispersive X-ray spectroscopy (EDX) in the scanning transmission electron microscope (STEM) is not likely to have sufficient resolution for this purpose, but it is suggested that the use of an atom probe could be appropriate.

There remains a problem with the paraequilibrium mode for purely reconstructive transformations, which does not appear to have received much attention. It arises because the definition of paraequilibrium appears to prohibit the necessary mass transport, for the following reason. During a reconstructive transformation, as already noted, the solute and solvent atoms must in general have atomic mobility both within and outside the interface itself. Atomic mobility within the interface accomplishes the destruction and reconstruction of the parent and product lattices respectively. The necessity for atomic mobility outside the interface depends upon the type of interfacial structure envisaged. If the Bain strain is assumed to represent the lattice correspondence between austenite and ferrite, then it can be shown[6] that the α/γ interface must be either incoherent or semicoherent. For sizable α particles, it cannot be fully coherent. This applies whether the transformation mechanism is reconstructive or displacive. If the α/γ interface is semicoherent, atomic mobility outside the interface is necessary because some of the misfit dislocations which maintain semicoherency have to climb normal to the interface. Regardless of whether the α/γ interface is incoherent or semicoherent, atomic mobility outside the interface is necessary because there is a volume change (4%) associated with the stress free α–γ transformation. This difference must be compensated for by a flux of

Table 4 Values of nucleation constants, assuming nucleation and growth by paraequilibrium mode of transformation: from Fig. 6*a*, $Q = (5{\cdot}9 \pm 1{\cdot}3) \times 10^{-19}$ J atom^{-1} and value of K_1^f derived from Fig. 6*b* is used throughout rest of work

Fig. no.	Fraction supporting nucleation K_1		Shape factor K_2
	Average	Standard error	
6*a*	$K_1^f = 4 \times 10^{-8}$	$K_1^f = 1 \times 10^{-12}$–$1 \times 10^{-3}$	...
6*b*	$K_1^f = 6{\cdot}9 \times 10^{-8}$	$K_1^f = 3{\cdot}1 \times 10^{-8}$–$1{\cdot}5 \times 10^{-7}$	$K_2^f = (2{\cdot}7 \pm 0{\cdot}6) \times 10^{-3}$
6*c*	$K_1^e = 1{\cdot}3 \times 10^{-8}$	$K_1^e = 1{\cdot}8 \times 10^{-9}$–$8{\cdot}9 \times 10^{-8}$	$K_2^e = (1{\cdot}0 \pm 0{\cdot}3) \times 10^{-3}$
6*d*	$K_1^c = 1{\cdot}2 \times 10^{-10}$	$K_1^c = 2{\cdot}1 \times 10^{-11}$–$7{\cdot}0 \times 10^{-10}$	$K_2^c = (3{\cdot}3 \pm 0{\cdot}5) \times 10^{-3}$

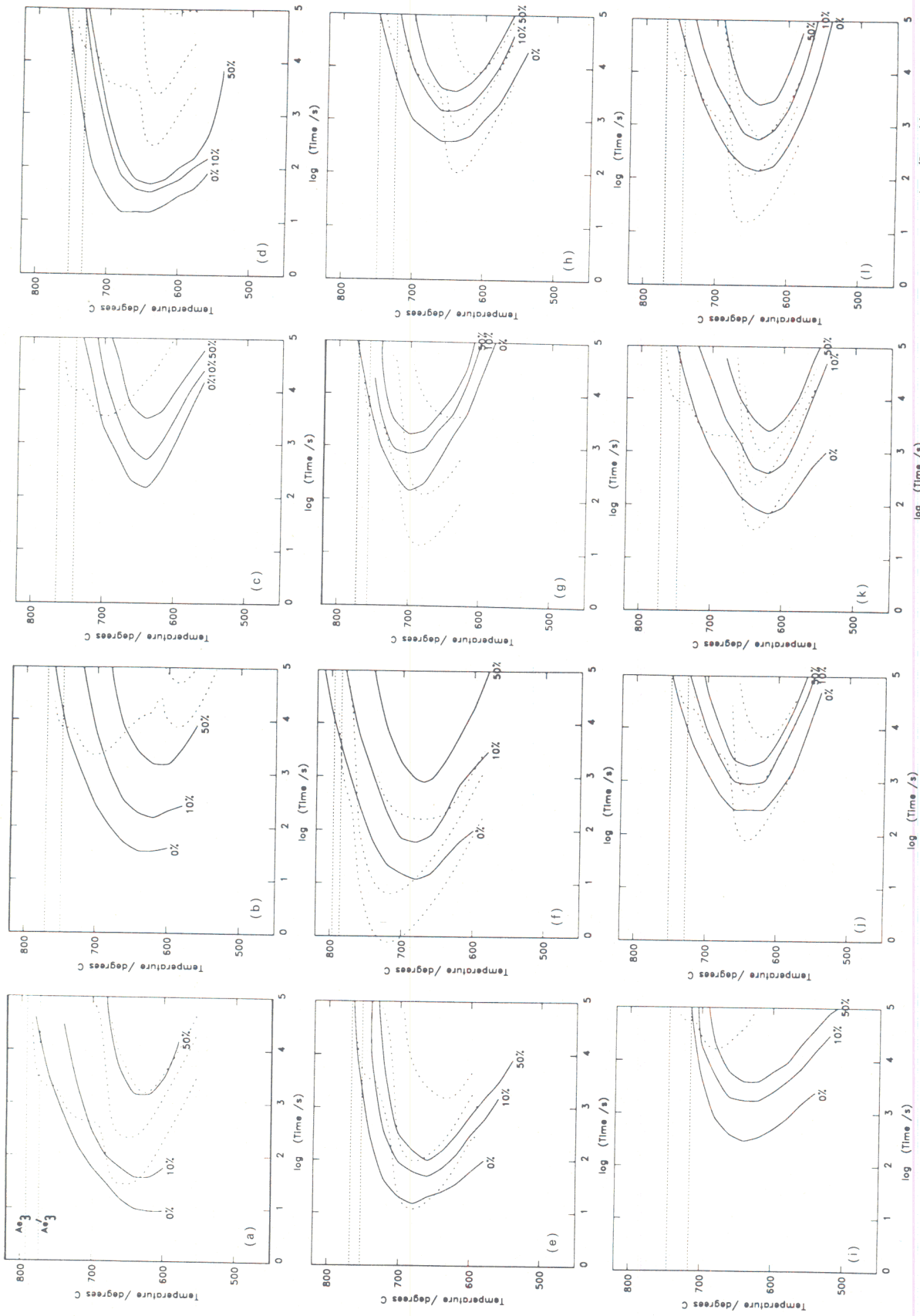

a En 13; *b* En 16; *c* En 17; *d* En 18; *e* En 19; *f* En 20 (ASTM 8); *g* En 20 (ASTM 7·5); *h* En 24; *i* En 100; *j* En 110; *k* En 354; *l* En 355

7 Observed (solid lines) and calculated (dotted lines) C-curves for the steels analysed in present work (*see* Table 1): calculations performed assuming equilibrium mode of transformation

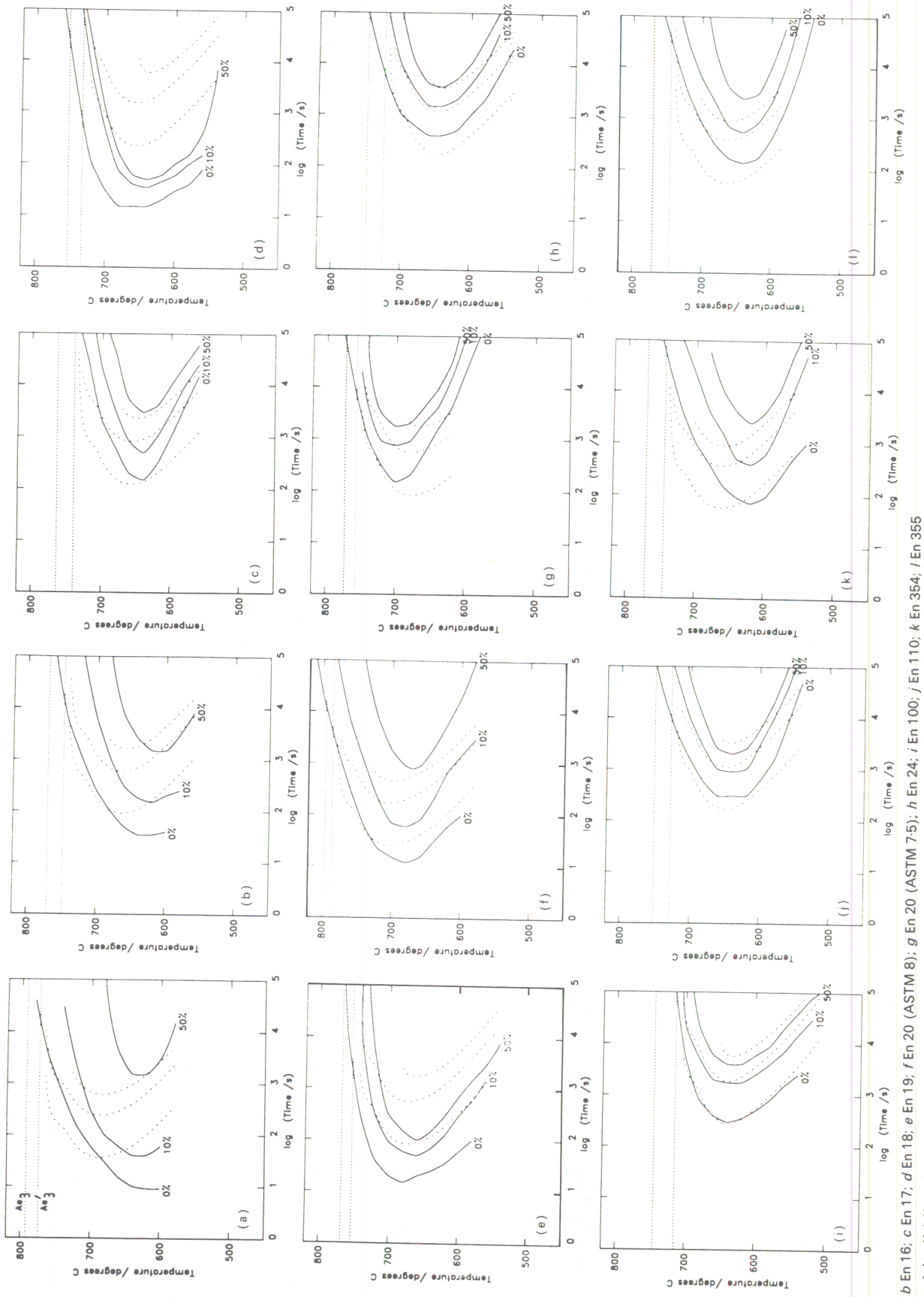

8 Observed (solid lines) and calculated (dotted lines) C-curves for the steels analysed in present work (*see* Table 1): calculations performed assuming paraequilibrium mode of transformation

a En 13; *b* En 16; *c* En 17; *d* En 18; *e* En 19; *f* En 20 (ASTM 8); *g* En 20 (ASTM 7·5); *h* En 24; *i* En 100; *j* En 110; *k* En 354; *l* En 355

vacancies between the growing precipitate and the dislocations, grain boundaries, and (ultimately) the free surface of the parent phase. The problem then arises that the reconstructive transformation requires atomic mobility outside the interface and yet, by the definition of paraequilibrium, the substitutional alloying elements should be configurationally frozen and thus unable to redistribute during transformation. Since the self-diffusivity of iron in austenite is at least comparable to or less than the diffusivities of substitutional elements,[27] it is probable that the iron atoms are also configurationally frozen.

Summary

The thermodynamic model used in this work (*see* Appendix) has been coupled with simplified kinetic theory, so that, subject to a number of assumptions, the one-dimensional parabolic thickening constant α_1 for the growth of allotriomorphic ferrite from supersaturated austenite can be estimated. This can be done assuming either the local equilibrium or the paraequilibrium mode of transformation.

To model the transformation from an input of the steel chemistry only, it is necessary to have a knowledge of the nucleation kinetics. Unfortunately, this is the least well understood part of the transformation and so, in this work, an indirect method has been used to deduce a suitable nucleation function. This involves using a simple model for the nucleation and growth of allotriomorphs as discs on the prior austenite boundary and the examination of experimental TTT curves. A form of equation consistent with classical nucleation theory was used and the resulting nucleation function should in theory be applicable across the compositional range of low alloy steels.

It is shown that the nucleation function derived assuming local equilibrium with respect to all components is unreasonable, as are the shapes of the calculated TTT diagrams. On the other hand, the nucleation function and the shapes of the TTT curves calculated assuming the paraequilibrium mode are more reasonable. For this reason, this work suggests that at temperatures only slightly below the Ae'_3 austenite decomposes to allotriomorphic ferrite by paraequilibrium transformation and that this growth mode operates over a large part of the observed range of transformation. At temperatures near the Ae'_3 partitioning of substitutional elements becomes more feasible and at temperatures between Ae'_3 and Ae_3 it becomes a thermodynamic necessity if transformation is to occur.

Finally, it is pointed out that there is a problem associated with the paraequilibrium mode of transformation, as applied to reconstructive transformations. It occurs because the paraequilibrium mode appears to preclude the reconstructive diffusion that is necessary to accomplish a stress free transformation.

Acknowledgments

One of the authors (RCR) would like to thank the Science and Engineering Research Council (SERC) and the National Power Technology and Environment Centre (NPTEC) for financial support in the form of an SERC/CASE studentship. The contribution of the other author (HKDHB) to this work was carried out under the auspices of the 'Atomic arrangements: design and control' project, which is a collaboration between the University of Cambridge and the Research and Development Agency of Japan. The authors are grateful to Professor D. Hull, FRS for the provision of laboratory facilities at the University of Cambridge.

References

1. 'Thermocalc' databank (*see*, for example, B. Sundman, Report D53, 'Summary of the modules in Thermocalc', The Royal Institute of Technology, Stockholm, Sweden, 1984).
2. 'Mtdata' (NPL metallurgical and thermochemical databank), National Physical Laboratory, Teddington, Middlesex.
3. R. C. REED: PhD thesis, University of Cambridge, 1990.
4. J. S. KIRKALDY and D. J. YOUNG: 'Diffusion in the condensed state'; 1987, London, The Institute of Metals.
5. H. K. D. H. BHADESHIA: *Prog. Mater. Sci.*, 1985, **29**, 321–386.
6. J. W. CHRISTIAN: 'The theory of transformations in metals and alloys', Part 1, 2 edn; 1975, Oxford, Pergamon Press.
7. J. S. KIRKALDY: *Can. J. Phys.*, 1958, **36**, 907–916.
8. G. R. PURDY, D. H. WEICHERT, and J. S. KIRKALDY: *Trans. AIME*, 1964, **230**, 1025–1034.
9. D. E. COATES: *Metall. Trans.*, 1972, **3**, 1203–1212.
10. D. E. COATES: *Metall. Trans.*, 1973, **4**, 395–396.
11. D. E. COATES: *Metall. Trans.*, 1973, **4**, 1077–1086.
12. D. E. COATES: *Metall. Trans.*, 1973, **4**, 2313–2325.
13. R. T. DeHOFF: in Proc. Int. Conf. on 'Solid–solid phase transformations', 503–520; 1981, Warrendale, PA, The Metallurgical Society of AIME.
14. J. R. BRADLEY and H. I. AARONSON: *Metall. Trans.*, 1981, **12A**, 1729–1741.
15. H. I. AARONSON and J. R. BRADLEY: *Trans. AIME*, 1966, **236**, 781–796.
16. J. S. KIRKALDY and G. R. PURDY: *Can. J. Phys.*, 1962, **40**, 208–217.
17. L. C. BROWN and J. S. KIRKALDY: *Trans. AIME*, 1964, **230**, 223–226.
18. C. WELLS, W. BATZ, and R. F. MEHL: *Trans. AIME*, 1950, **188**, 553–560.
19. R. P. SMITH: *Acta Metall.*, 1953, **1**, 578–587.
20. R. TRIVEDI and G. M. POUND: *J. Appl. Phys.*, 1967, **38**, 3569–3576.
21. R. H. SILLER and R. B. McLELLAN: *Trans. AIME*, 1969, **245**, 697–700.
22. R. H. SILLER and R. B. McLELLAN: *Metall. Trans.*, 1970, **1**, 985–988.
23. R. B. McLELLAN and W. DUNN: *J. Phys. Chem. Solids*, 1969, **30**, 2631–2637.
24. W. DUNN and R. B. McLELLAN: *Metall. Trans.*, 1970, **1**, 1263–1265.
25. H. K. D. H. BHADESHIA: *Met. Sci.*, 1981, **15**, 477–479.
26. H. K. D. H. BHADESHIA: *Met. Sci.*, 1981, **15**, 178–180.
27. J. FRIDBERG, L. TORNDAHL, and M. HILLERT: *Jernkontorets Ann.*, 1969, **153**, 263–276.
28. G. BOLZE, D. E. COATES, and J. S. KIRKALDY: *Trans. ASM*, 1969, **62**, 794–803.
29. A. HULTGREN: *Jernkontorets Ann.*, 1951, **135**, 403–483.
30. M. HILLERT: *Jernkontorets Ann.*, 1952, **136**, 25–37.
31. H. I. AARONSON, H. A. DOMIAN, and G. M. POUND: *Trans. AIME*, 1966, **236**, 768–781.
32. 'BISRA atlas of isothermal transformation diagrams of BS En steels', Special Report no. 56, 2 edn, 1956, London, The Iron and Steel Institute.
33. M. ENOMOTO: *Trans. Iron Steel Inst. Jpn*, 1988, **28**, 826–835.
34. H. K. D. H. BHADESHIA, L.-E. SVENSSON, and B. GRETOFT: in 'Proceedings of an international conference on welding metallurgy of structural steels', (ed. J. Y. Koo); 1987, Warrendale, PA, The Metallurgical Society of AIME.
35. J. R. BRADLEY, J. M. RIGSBEE, and H. I. AARONSON: *Metall. Trans.*, 1977, **8A**, 323–333.
36. J. W. CAHN: *Acta Metall.*, 1956, **4**, 449–459.
37. M. AVRAMI: *J. Chem. Phys.*, 1939, **7**, 1103–1112.
38. W. C. JOHNSON *et al.*: *Metall. Trans.*, 1975, **6A**, 911–919.
39. W. F. LANGE, M. ENOMOTO, and H. I. AARONSON: *Metall. Trans.*, 1988, **19A**, 427–440.
40. J. S. KIRKALDY and E. A. BAGANIS: *Metall. Trans.*, 1978, **9A**, 495–501.
41. G. F. VAN DER VOORT: 'Metallography: principles and practices'; 1984, New York, McGraw-Hill.
42. F. E. BOWMAN: *Trans. ASM*, 1946, **36**, 61–80.

43. H. I. AARONSON and H. A. DOMIAN: *Trans. AIME*, 1966, **236**, 781–796.
44. M. ENOMOTO and H. I. AARONSON: *Metall. Trans.*, 1987, **18A**, 1547–1557.
45. M. ENOMOTO: *Metall. Trans.*, 1989, **20A**, 332–333.
46. H. K. D. H. BHADESHIA: *Metall. Trans.*, 1989, **20A**, 333–334.

Appendix

The thermodynamic model employed here is a modified form of the work of Hashiguchi *et al.*[47] The method allows the accurate prediction of Fe–C base multicomponent phase diagrams, provided that the total substitutional alloying content is less than 5 wt-% and the silicon content is less than 1 wt-%. This limitation on composition arises because the logarithm of the activity coefficient of each solute is expressed as a Taylor series in the mole fractions of solutes present:[48] following the Wagner formalism, terms of order greater than unity are neglected. The formalism is expected to fail for highly alloyed steels, when solutes are expected to interact strongly. There is, however, an advantage in using the Wagner formalism for the purpose of the present work, because the cross-terms in the diffusivity matrix are a function of the Wagner interaction parameters (equation (16)) and can therefore be evaluated readily.

Since the accuracy of all thermodynamic models depends ultimately upon the reliability of the experimental data used to calibrate it, as well as the type of model, an effort has been made to examine and evaluate the available data.

Gibbs energy change for ferrite–austenite transformation of pure iron

In the model of Hashiguchi *et al.*, the effect of an alloying element i on the relative stability of austenite and ferrite is expressed by the term $\Delta G_0^{\circ,\alpha\rightarrow\gamma}$ which represents[49] the free energy change for the transfer of one mole of solute i from ferrite to austenite, in the limiting case of an alloy of pure iron.

Since the present work is concerned with low alloy steels, it is important that $\Delta G_i^{\circ,\alpha\rightarrow\gamma}$ $(i=0)$ is known reliably. Values have been measured by several investigators, e.g. Refs. 50, 51. More recent evaluations (e.g. Refs. 52–54) have been based upon 'optimising' the existing data.

On examination of the above data, it becomes apparent that between 750 and 950°C the data are consistent within ~ 20 J mol^{-1}. However, below 500°C, the data of Kaufman and co-workers diverge from that of Orr and Chipman[52] and Agren;[54] at 400°C, they differ by >300 J mol^{-1}. In a review of the available thermodynamic data, Bhadeshia[55] came to the conclusion that the data of Kaufman and co-workers[50,51] are well established, reliable, and accurate for low temperature applications. This tabulation was used throughout the present work.

Gibbs energy change for ferrite–austenite transformation of substitutional solutes

A large part of the thermodynamic dataset of Hashiguchi *et al.* was evaluated by considering the Uhrenius[56] adaptation of the regular solution model derived by Hillert and Staffanson.[57] According to the Uhrenius subregular solution model, $\Delta G_i^{\circ,\alpha\rightarrow\gamma}$ is given by the expression

$$\Delta G_i^{\circ,\alpha\rightarrow\gamma} = G_i^{\circ,\gamma} - G_i^{\circ,\alpha} + {}^0L_{0i}^{V,\gamma} + {}^1L_{0i}^{V,\gamma} + {}^0L_{0i}^{V,\alpha} + {}^1L_{0i}^{V,\alpha} \quad \ldots\ldots\ldots (50)$$

where the terms in G_i° represent the standard molar free energies of the component i and the terms in L are interaction parameters. For example, ${}^0L_{0i}^{V,\gamma}$ and ${}^1L_{0i}^{V,\gamma}$ are interaction parameters representing the iron–substitutional interaction in austenite, when all interstitial sites are filled with vacancies.

The terms $\Delta G_i^{\circ,\alpha\rightarrow\gamma}$ can be evaluated by substitution of Uhrenius data into equation (50), which does not appear in the paper of Hashiguchi *et al.*[47] The results are presented in Table 5 and correct a number of typographical errors in the work of Hashiguchi *et al.* A typographical error in the Uhrenius[56] paper is taken into account. The term $(S_{Fe}^{\circ,\alpha})_{mag}$ is the magnetic contribution to the Gibbs free energy change of pure iron.[58,59] The tabulation from Kaufman and co-workers[50,51] has been used for this term for the sake of consistency, because the tabulation due to these workers has been chosen for $\Delta G_0^{\circ,\alpha\rightarrow\gamma}$.

Gibbs energy change for ferrite–austenite transformation of carbon

Following Kirkaldy and Baganis,[40] $\Delta G_1^{\circ,\alpha\rightarrow\gamma}$ (in J mol^{-1}) is evaluated according to the expression

$$\Delta G_1^{\circ,\alpha\rightarrow\gamma} = -64\,111{\cdot}4 + 32{\cdot}158T \quad \ldots\ldots (51)$$

where T is expressed in Kelvin.

Calculation of Wagner interaction parameters for substitutional solutes

The Wagner interaction parameters are defined by the expressions[60,61]

$$\varepsilon_{11} = \left(\frac{\partial \ln\{\Gamma_1\}}{\partial x_1}\right)_{x_0\rightarrow 1} \quad \ldots\ldots (52)$$

$$\varepsilon_{1i} = \left(\frac{\partial \ln\{\Gamma_1\}}{\partial x_i}\right)_{x_0\rightarrow 1} \quad \ldots\ldots (53)$$

$$\varepsilon_{i1} = \left(\frac{\partial \ln\{\Gamma_i\}}{\partial x_1}\right)_{x_0\rightarrow 1} \quad \ldots\ldots (54)$$

$$\varepsilon_{ii} = \left(\frac{\partial \ln\{\Gamma_i\}}{\partial x_i}\right)_{x_0\rightarrow 1} \quad \ldots\ldots (55)$$

where Γ_1 and Γ_i represent the activity coefficients of carbon and substitutional solute i.

Following Hashiguchi *et al.*, $\ln\{\Gamma_1\}$ and $\ln\{\Gamma_i\}$ are evaluated according to the Uhrenius subregular solution model. The appropriate expressions are

$$\ln\{\Gamma_1\} = -\ln\{-x_1 + c(1-x_1)\} + G_1^E/(RT) \quad \ldots (56)$$

$$\ln\{\Gamma_i\} = -\ln\{1-x_1\} + c\ln\{1-x_1/[c(1-x_1)]\} + G_i^E/(RT) \quad \ldots\ldots (57)$$

Table 5 Gibbs free energy change per mole of substitutional solute passing from $\alpha\rightarrow\gamma$, in limiting case of pure iron: $(S_{Fe}^{\circ,\alpha})_{mag}$ is magnetic contribution to free energy change and temperature T is expressed in Kelvin

Element	$\Delta G_i^{\circ,\alpha\rightarrow\gamma}$, J mol^{-1}
Mn	$-20\,520 + 4{\cdot}086T + 1500(S_{Fe}^{\circ,\alpha})_{mag}$
Si	$7087 - 4{\cdot}127T$
Ni	$-12\,950 + 5{\cdot}02T + 383(S_{Fe}^{\circ,\alpha})_{mag}$
Cr	$-1534 - 19{\cdot}472T + 2{\cdot}74T\ln T$
Mo	$310 - 0{\cdot}284T + 400(S_{Fe}^{\circ,\alpha})_{mag}$

where T is the temperature, R is the gas constant, and c is the ratio of interstitial to substitutional sites available; thus $c = 1$ for austenite and $c = 3$ for ferrite. The terms G_1^E and G_i^E are excess energies, which can be evaluated by the expressions and data in Ref. 56.

Combining equations (52)–(57)

$$\varepsilon_{11} = \frac{c+1}{c} + \frac{1}{RT}\left(\frac{\partial G_1^E}{\partial x_1}\right)_{x_0 \to 1} \quad \ldots\ldots\ldots (58)$$

$$\varepsilon_{1i} = \frac{1}{RT}\left(\frac{\partial G_1^E}{\partial x_i}\right)_{x_0 \to 1} \quad \ldots\ldots\ldots (59)$$

$$\varepsilon_{i1} = \frac{1}{RT}\left(\frac{\partial G_i^E}{\partial x_1}\right)_{x_0 \to 1} \quad \ldots\ldots\ldots (60)$$

$$\varepsilon_{ii} = \frac{1}{RT}\left(\frac{\partial G_i^E}{\partial x_i}\right)_{x_0 \to 1} \quad \ldots\ldots\ldots (61)$$

Thus, using equations (58)–(61), the Wagner interaction parameters can be calculated by differentiation and by then taking the limiting case of pure iron. Expressions for Wagner interaction parameters derived in this way are given in Table 6. Expressions calculated for parameters involving nickel and silicon differ from those reported by Hashiguchi *et al.*[47] In addition, expressions for the carbon substitutional terms in ferrite are included; these do not feature in Ref. 47.

Calculation of Wagner interaction parameters for carbon

An attempt has been made to calibrate the thermodynamic model used here against the calculation of the Fe–C binary carried out by Bhadeshia[62] using the quasichemical theory developed by Lacher,[63] Fowler and Guggenheim,[64] and McLellan and Dunn.[23] Quasichemical models have received considerable attention in the literature (e.g. Refs. 62, 65); they represent attempts to model departures from an ideal entropy of mixing. The $\gamma/(\gamma+\alpha)$ and $\alpha/(\gamma+\alpha)$ phase boundaries can then be extrapolated beyond the eutectoid temperature with greater confidence. The calibration has been carried out as follows.

The condition of equipotential for carbon at equilibrium can be expressed by

$$\Delta G_0^{\circ,\alpha\to\gamma} = RT \ln\left\{\frac{x_0^\alpha \Gamma_0^\alpha}{x_0^\gamma \Gamma_0^\gamma}\right\} \quad \ldots\ldots\ldots (62)$$

$$\Delta G_1^{\circ,\alpha\to\gamma} = RT \ln\left\{\frac{x_1^\alpha \Gamma_1^\alpha}{x_1^\gamma \Gamma_1^\gamma}\right\} \quad \ldots\ldots\ldots (63)$$

The activity coefficients for the binary Fe–C system, written in terms of the Wagner interaction parameters, are given by the expressions[47]

$$\ln\{\Gamma_0^\gamma\} = -\tfrac{1}{2}\varepsilon_{11}^\gamma x_1^\gamma x_1^\gamma \quad \ldots\ldots\ldots (64)$$

$$\ln\{\Gamma_0^\alpha\} = -\tfrac{1}{2}\varepsilon_{11}^\alpha x_1^\alpha x_1^\alpha \quad \ldots\ldots\ldots (65)$$

$$\ln\{\Gamma_1^\gamma\} = \varepsilon_{11}^\gamma x_1^\gamma \quad \ldots\ldots\ldots (66)$$

$$\ln\{\Gamma_1^\alpha\} = \varepsilon_{11}^\alpha x_1^\alpha \quad \ldots\ldots\ldots (67)$$

Assuming the x_1^α and x_1^γ values calculated by Bhadeshia,[62]

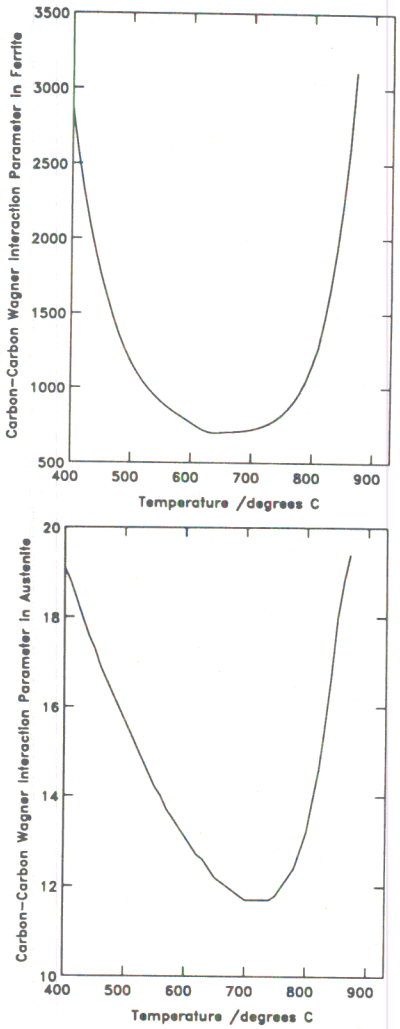

9 Variation of carbon–carbon Wagner interaction parameters in ferrite and austenite as function of temperature

the unknowns are the Wagner interaction parameters ε_{11}^γ and ε_{11}^α. These can be calculated by combining equations (62)–(67) to arrive at the expressions

$$\varepsilon_{11}^\gamma = \frac{2}{(x_1^\gamma - x_1^\alpha)x_1^\gamma}\left(\frac{\Delta G_0^{\circ,\alpha\to\gamma}}{RT} - \ln\left\{\frac{x_0^\alpha}{x_0^\gamma}\right\}\right) + \frac{x_1^\alpha}{(x_1^\gamma - x_1^\alpha)x_1^\gamma}\left(\frac{\Delta G_1^{\circ,\alpha\to\gamma}}{RT} - \ln\left\{\frac{x_1^\alpha}{x_1^\gamma}\right\}\right) \quad \ldots (68)$$

$$\varepsilon_{11}^\alpha = \frac{2}{(x_1^\gamma - x_1^\alpha)x_1^\alpha}\left(\frac{\Delta G_0^{\circ,\alpha\to\gamma}}{RT} - \ln\left\{\frac{x_0^\alpha}{x_0^\gamma}\right\}\right) + \frac{x_1^\gamma}{(x_1^\gamma - x_1^\alpha)x_1^\alpha}\left(\frac{\Delta G_1^{\circ,\alpha\to\gamma}}{RT} - \ln\left\{\frac{x_1^\alpha}{x_1^\gamma}\right\}\right) \quad \ldots (69)$$

This procedure ensures that the binary Fe–C phase diagram is equivalent to that calculated from the quasichemical model. The values of the Wagner interaction parameters calculated in this way are shown in Fig. 9.

Table 6 Expressions derived for Wagner interaction parameters

Element	ε_{ii}^γ	ε_{ii}^α	ε_{i1}^γ	ε_{i1}^α
Mn	$2{\cdot}406 - 175{\cdot}6/T$	$3{\cdot}082 - 4679/T + 360{\cdot}8(S_{Fe}^{\circ,\alpha})_{mag}/T$	$-4811/T$	$-5834/T$
Si	$26\,048/T$	$-16{\cdot}35 + 44\,829/T$	$14\,795/T$	$16\,205/T$
Ni	$-2839/T$	$2{\cdot}013 - 4595/T + 92{\cdot}1(S_{Fe}^{\circ,\alpha})_{mag}/T$	$5533/T$	$5533/T$
Cr	$7{\cdot}655 - 3154/T - 0{\cdot}661 \ln\{T\}$	$2{\cdot}819 - 6039/T$	$14{\cdot}19 - 30\,210/T$	$1{\cdot}558 - 6160/T$
Mo	$-2330/T$	$-0{\cdot}219 - 4772/T + 96{\cdot}2(S_{Fe}^{\circ,\alpha})_{mag}/T$	$-10\,714/T$	$-10\,714/T$

Method of solution

The method used here for the calculation of equilibrium and paraequilibrium tielines has been described fully by Hashiguchi *et al.*[47]

An additional requirement here is the calculation of the driving force per unit volume ΔG_V associated with the formation of a critical nucleus of ferrite, the composition of which differs from that of ferrite at equilibrium because of the capillarity effect. Assuming that the partial molar volumes of iron, carbon, and substitutional solutes are equal, the parallel tangent construction takes into account this effect. The driving force calculated in this way corresponds to the *maximum* value of ΔG_V. Enomoto and Aaronson[66] have shown that calculated values of ΔG_V are changed only slightly when the variation in partial molar volumes is taken into account. Therefore, it seems reasonable to employ the parallel tangent construction throughout the present work.

Assuming that substitutional solutes as well as carbon can partition during nucleation, the composition of the ferrite nucleus is given by solving the equations

$$\mu_0^{\gamma} - \mu_0^{\alpha,\mathrm{nuc}} = \mu_1^{\gamma} - \mu_1^{\alpha,\mathrm{nuc}} = \mu_i^{\gamma} - \mu_i^{\alpha,\mathrm{nuc}} \quad \text{for } i = 2 \rightarrow n \qquad (70)$$

where $\mu_0^{\alpha,\mathrm{nuc}}$, $\mu_1^{\alpha,\mathrm{nuc}}$, and $\mu_i^{\alpha,\mathrm{nuc}}$ refer to the chemical potentials of iron, carbon, and substitutional solute i in the ferrite nucleus, and μ_0^{α}, μ_1^{α}, and μ_i^{α} refer to the chemical potentials in the bulk austenite. Equation (70) can be solved by only a slightly modified version of the model derived by Hashiguchi *et al.*

Under paraequilibrium conditions, the nucleus composition is given by solving the equations

$$x_0^{\gamma}(\mu_0^{\gamma} - \mu_0^{\alpha,\mathrm{nuc}}) + \sum_{i=2}^{n} x_i^{\gamma}(\mu_i^{\gamma} - \mu_i^{\alpha,\mathrm{nuc}}) = x_1^{\gamma}(\mu_1^{\gamma} - \mu_1^{\alpha,\mathrm{nuc}}) \qquad (71)$$

under the constraint

$$\frac{x_i^{\gamma}}{1 - x_1^{\gamma}} = \frac{x_i^{\alpha}}{1 - x_1^{\alpha}} = \frac{\bar{x}_i}{1 - \bar{x}_1} \quad \text{for } i = 2 \rightarrow n \qquad (72)$$

For both the equilibrium as well as the paraequilibrium mode of transformation, ΔG_V is given by

$$\Delta G_V = \frac{x_0^{\gamma}(\mu_0^{\alpha,\mathrm{nuc}} - \mu_0^{\gamma}) + x_1^{\gamma}(\mu_1^{\alpha,\mathrm{nuc}} - \mu_1^{\gamma}) + \sum_{i=2}^{n} x_i^{\gamma}(\mu_i^{\alpha,\mathrm{nuc}} - \mu_i^{\gamma})}{\bar{V}} \qquad (73)$$

where $\bar{V}$ is the molar volume, which is taken as $7{\cdot}2 \times 10^{-6}$ m^3 mol^{-1}.

References

47. K. HASHIGUCHI, J. S. KIRKALDY, T. FUKUZUMI, and V. PAVASKER: *Calphad*, 1984, **8**, 173–186.
48. C. H. P. LUPIS: 'Chemical thermodynamics of materials'; 1983, Amsterdam/New York, Elsevier Science.
49. M. HILLERT, T. WADA, and H. WADA: *J. Iron Steel Inst.*, 1967, **205**, 539–546.
50. L. KAUFMAN, E. V. CLOUGHERTY, and R. J. WEISS: *Acta Metall.*, 1963, **11**, 323–335.
51. L. KAUFMAN and H. BERNSTEIN: in 'Refractory materials', Vol. 4, 'Computer calculation of phase diagrams; with special reference to refractory metals'; 1970, New York, Academic Press.
52. R. L. ORR and J. CHIPMAN: *Trans. AIME*, 1967, **239**, 630–633.
53. M. HILLERT and M. JARL: *Calphad*, 1978, **2**, 227–238.
54. J. AGREN: *Metall. Trans.*, 1979, **10A**, 1847–2065.
55. H. K. D. H. BHADESHIA: *Mater. Sci. Technol.*, 1985, **1**, 497–504.
56. B. UHRENIUS: in 'Hardenability concepts with applications to steel', (ed. D. V. Doane and J. S. Kirkaldy), 28–81; 1978, Pittsburgh, PA, AIME.
57. M. HILLERT and L.-I. STAFFANSON: *Acta Chem. Scand.*, 1970, **24**, 3618–3626.
58. R. J. WEISS and K. J. TAUER: *Phys. Rev.*, 1956, **102**, 1490–1495.
59. C. ZENER: *Trans. AIME*, 1955, **203**, 619–630.
60. C. WAGNER: 'Thermodynamics of alloys', 47–53; 1952, Reading, MA, Addison-Wesley.
61. J. CHIPMAN: *J. Iron Steel Inst.*, 1955, **180**, 97–106.
62. H. K. D. H. BHADESHIA: *Met. Sci.*, 1982, **16**, 167–169.
63. J. R. LACHER: *Proc. Cambridge Philos. Soc.*, 1937, **33**, 518–523.
64. R. H. FOWLER and E. A. GUGGENHEIM: 'Statistical thermodynamics'; 1939, New York, Cambridge University Press.
65. G. J. SHIFLET, J. R. BRADLEY, and H. I. AARONSON: *Metall. Trans.*, 1978, **9A**, 999–1008.
66. M. ENOMOTO and H. I. AARONSON: *Metall. Trans.*, 1986, **17A**, 1381–1384.